Lipid membranes modulate the activity of RNA through sequence-dependent interactions

Authors: Tomasz Czerniak[a] and James P Saenz[a]*

[a] Technische Universität Dresden, B CUBE Center for Molecular Bioengineering, 01307 Dresden, Germany

*corresponding author and lead contact: james.saenz@tu-dresden.de

Abstract

RNA is a ubiquitous biomolecule that can serve as both catalyst and information carrier. Understanding how RNA activity is controlled and how it in turn regulates bioactivity is crucial for elucidating its physiological roles and potential applications in synthetic biology. Here we show that lipid membranes can act as RNA organization platforms, introducing a novel mechanism for ribo-regulation. The activity of R3C ribozyme can be modified by the presence of lipid membranes, with direct RNA-lipid interactions dependent on RNA nucleotide content, base pairing and length. In particular, the presence of guanine in short RNAs is crucial for RNA-lipid interactions, while double-stranded RNAs further increase lipid-binding affinity. Lastly, by artificially modifying the R3C substrate sequence to enhance membrane binding we generated a lipid-sensitive ribozyme reaction with riboswitch-like behavior. These findings introduce RNA-lipid interactions as a tool for developing synthetic riboswitches and novel RNA-based lipid biosensors, and bear significant implications for RNA World scenarios for the origin of life.

Introduction

RNA performs diverse functions ranging from information storage to regulation of other biomolecules and direct catalysis of biochemical reactions. The functional versatility of RNA has implications for understanding plausible scenarios for the origin of life[1–3], and for developing tools in synthetic biology[4–6]. Research aimed at understanding how an RNA World could have emerged has motivated development of ribozymes with functions including RNA ligation[7–10], replication[11,12] and other activities[13–16]. The experimental development of functional RNAs raises the possibility of RNA-based synthetic systems. For both synthetic life and understanding the origin of self-replicating organisms, RNA has intrinsic appeal: it can serve functions of both DNA (information storage) and proteins (enzymes), obviating the need for translation machineries and protein chaperones. Furthermore, RNA does not undergo irreversible denaturation like proteins, lending robustness against a broad range of physical and chemical conditions. In order to design a system based on RNA, however, it is essential to be able to coordinate RNA activity in space and time.

Key to harnessing the functional versatility of RNA is understanding how to spatially and temporally modulate its properties and to selectively modulate the activity of different RNAs within one system. The physicochemical environment surrounding an RNA molecule is a central determinant of its structure, stability and activity. Spontaneous RNA hydrolysis and ligation, as well as catalytic RNA activity are sensitive to pH[17], ionic strength[18,19] and RNA concentration changes[11], among other parameters. Similarly, RNA activity can be modulated by interactions with molecules such as ions,

proteins, and other nucleic acids[20]. Thus, one approach to regulating RNA activity could be via tunable interactions with binding partners that affect RNA structure, concentration or chemical microenvironment.

One mechanism for modulating RNA activity could be through direct RNA-lipid interactions[19,21,22]. Because of their amphiphilic nature, lipids spontaneously self-assemble into membranous structures that can encapsulate RNA into protected and selective microcompartments[23–25]. Alternatively, direct RNA-lipid interactions could localize RNAs to membrane surfaces, increasing its local concentration and reducing dimensionality for intermolecular interactions[21]. Lastly, localization to a lipid surface brings RNA into a physicochemically unique microenvironment with sharp gradients of hydrophobicity, electrical permittivity, and water activity. Through these effects, RNA-lipid interactions could provide a powerful mechanism for modulating RNA activity.

The first functional RNA-lipid interaction was described more than 40 years ago[26], with subsequent research revealing various factors that facilitate nucleic acid-lipid binding[27–37]. More recently, specific RNA sequences have been generated through SELEX with affinity for fluid membranes comprised of phospholipids and cholesterol[38–40]. Interestingly, mixtures of RNAs have also been shown to bind to membranes that are in a solid crystalline (gel) phase[41,42]. These studies revealed that, while most randomized mixtures of RNA sequences can bind to gel membranes, there is a relatively small chemical space of oligomers that have affinity for fluid membranes. Thus, conceptually, gel membranes could provide a platform for modulating the activity of a diverse range of RNAs. However, the effects of gel membranes on RNA activity and the sequence selectivity of such interactions are relatively unexplored.

This study reports the effect of lipid membranes on RNA catalytic activity. We show that RNA-lipid binding depends on the primary sequence, secondary structure, and length of RNA. Using the trans-acting R3C ligase ribozyme, we observed that R3C-lipid binding changes ribozyme activity in a concentration-dependent manner. Lipid binding assays show that the interaction of short RNA sequences with gel membranes depends on guanine content and the presence of double-stranded structures. Lastly, modification of R3C's substrate sequence increased the tunability of R3C-based reactions through a lipid-dependent mechanism. Our findings demonstrate that membranes can serve as platforms for ribo-regulation, which could contribute to the development of RNA-based lipid biosensors and lipid-sensitive riboswitches. This approach introduces new tools for molecular and synthetic biology and raises the prospect of previously unrecognized roles for RNA-lipid interactions in the origin and evolution of life.

Results

The discovery that RNA can catalyse reactions in addition to encoding information[18,43], opened new directions for engineering life and the possibility of protocells emerging from an RNA world[2]. But, a key missing ingredient for RNA-based systems is a mechanism to organize RNAs and regulate their activity. We hypothesized that RNA-membrane interactions could influence ribozyme activity by changing local RNA concentrations at the membrane surface or influencing RNA conformations.

To test the hypothesis that lipid membranes can serve as platforms for ribo-regulation, we took advantage of the observation that RNA can interact with solid crystalline (gel) phase membranes composed of phosphatidylcholine lipids[41,42]. To visibly demonstrate this phenomenon we prepared giant unilamellar vesicles (GUVs) that are phase separated into gel and liquid domains and we then

observed the distribution of a random mixture of RNA oligomers stained with SybrGold by fluorescence microscopy (**Fig. 1a**). A fluorescent lipid probe (DiD) was enriched in membrane liquid domains and was excluded from gel phase domains. In contrast, RNA was enriched within the gel phase domains. RNA enrichment on GUVs was reversed by heating the system above the gel phase melting temperature, resulting in an entirely liquid phase vesicle (**Fig. 1b**). Binding of RNA oligonucleotides to gel-phase small unilamellar vesicles (SUVs) can also lead to aggregation into large visible RNA-lipid assemblies (**Fig. 2a**) [27,35,41,42]. Depletion of divalent cations or increasing temperature above the lipid melting temperature (i.e. producing fluid instead of gel membranes) reduced RNA-membrane binding and aggregation (**Fig. 2a**). Taken together, reversible RNA-lipid binding and lipid-dependent aggregation could provide a tunable mechanism to concentrate and regulate RNAs in simple bottom up synthetic systems, or in a prebiotic environment.

RNA-lipid binding changes the probability of RNA-RNA interactions

To determine whether local RNA concentration is influenced by interaction with lipid membranes, we relied on UV-mediated crosslinking. All small vesicle membranes in this study were composed of dipalmitoylphosphatidylcholine (DPPC), which is in a solid crystalline (gel) phase at the experimental temperature of 24°C. Nucleic acid bases absorb UV light, producing chemical changes that yield base-base covalent bonds in a distance-dependent manner, yielding insights into the structure and interactions of nucleic acids[44–46]. We first observed the effect of gel membranes on the crosslinking of a single defined RNA sequence, the R3C ligase, which predominately forms one structure (R3C ligase, **Fig. 2d**). When subjected to UV, the R3C ligase shows slightly increased crosslinking in the presence of low lipid concentrations. A further increase in lipid concentration led to decreased crosslinking efficiency, possibly through dilution of the RNA species on the surface of the lipid membranes. This effect was inversely correlated with RNA-lipid binding efficiency (**Fig. 2b**). In contrast, a mixture of RNA oligomers with randomized sequences which is able to create a more diverse range of intermolecular structures (**Fig. 2d**) showed continuously increasing and overall higher UV-crosslinking efficiency in the presence of lipids (**Fig. 2c**). The contrasting effect of crosslinking for R3C and randomized oligomers might be explained by the influence of lipid membranes on RNA interactions: membrane binding could potentially stabilize base-pairing[47] and thereby enhance crosslinking efficiency, whereas the decrease of crosslinking might be caused by a dilution effect at higher membrane surface areas or by lipid-based steric hindrance. These observations demonstrate that RNA-membrane interactions can influence RNA-RNA interactions in a manner that is dependent on lipid concentration and RNA sequence diversity. This further suggests that membrane binding could have an effect on trans-acting ribozyme activity derived from base pairing.

RNA-lipid interactions influence RNA catalytic activity

To investigate the functional consequence of RNA-lipid binding, we tested the effect of lipids on the activity of the trans-acting R3C ligase ribozyme. R3C ligase is a relatively short ribozyme that catalyzes ligation of substrate strands to the ribozyme[10](**Fig. 3a**). Since R3C is also part of an RNA self-replication system [11,12], the effects of lipids on R3C are also interesting with regard to the emergence, evolution and artificial synthesis of autonomous self-replicating systems. The R3C reaction rate in the absence of membranes was 11 pM/min, with a reaction constant rate of $k = 6.4 \times 10^{-4}$ min^{-1}. Addition of lipid vesicles led to an increased reaction rate (14 pM/min, +29%), which could plausibly be due to increased ligase-substrate interaction on the membrane either through increased concentrations at the membrane surface or through stabilization of base pairing[47]. At the highest lipid concentration, the reaction rate dropped to 8 pM/min (-27%) (**Fig. 3b**). A decrease in reaction rate was correlated with

137 further R3C ligase binding to the lipid membranes (>100 lipid/R3C, **Fig. 2b**) and we speculate that this
138 may be caused by steric hindrance from the lipid vesicles. These results show that gel membranes can
139 influence the reaction rate of a trans-acting ribozyme in a lipid concentration-dependent manner.
140
141 **R3C ligase and its substrate bind differently to the membrane**
142 To further understand how R3C and substrate membrane binding might contribute to changes in
143 ligation rates, we analyzed lipid-binding affinities of the ligase and its substrate. To quantify binding to
144 the membranes, we calculated lipid–buffer partition coefficients (K). The partition coefficient of the
145 short 12 nt substrate was more than 3 orders of magnitude lower than that of the 84 nt R3C ligase (**Fig.**
146 **3c**). Thus, in this system, substrate-membrane binding is essentially negligible compared with R3C-
147 membrane binding. Combined with our observation that RNA-RNA interactions are stabilized by
148 membrane binding (**Fig. 2c**), this indicates that the increased activity observed in **Figure 3b** was due to
149 an effect of the membrane on the R3C ligase-substrate complex stability, rather than through
150 substrate-lipid interactions on the membrane surface. Thus, membranes can enhance ribozyme
151 activity by promoting the stability of reaction intermediates.
152
153 **RNA sequence influences binding to gel membranes**
154 Understanding the features that influence RNA-lipid interactions could allow us to engineer RNAs with
155 higher membrane affinity, and thereby potentially enhance activity by concentrating RNAs at the
156 membrane surface. Interactions of RNA with gel-phase membranes have been previously shown to
157 exhibit low sequence-dependence, based on binding of oligos with randomized sequences[41,42].
158 However, the large difference in binding for R3C and its substrate suggests that RNA-gel membrane
159 interactions might in fact be dependent on RNA composition or structure.
160
161 To investigate which features of RNA influence its interaction with lipid membranes we first evaluated
162 how base content influences membrane binding of short RNA species. 19nt oligomers with only one
163 type of nucleotide were tested together with a random sequence as a control. To quantify relative
164 changes of RNA-membrane binding, we calculated the RNA binding efficiency as a percentage of total
165 RNA bound to membranes at a fixed oligo-to-lipid ratio. Remarkably, whereas the 19xG oligomer
166 bound very efficiently to the gel-phase membrane (84% binding efficiency), oligomers of A, C or U
167 showed practically no binding. A mixture of 19-mer RNA with randomized sequences showed
168 moderate binding (33% binding efficiency), as did one with AG-repeats (**Fig. 4a**), most probably due to
169 the introduction of guanine. Guanine could conceivably enhance binding either through direct
170 interactions with the membrane, or alternatively by promoting G≡C base pairing or presence of G-
171 quadruplexes, thereby influencing structure. The enhanced binding of an oligomer with only AG-
172 repeats suggests that membrane binding can be influenced by direct guanine-membrane
173 interactions[48].
174
175 We next examined the effect of deleting a specific base from mixtures of 40-mer oligos with
176 randomized sequences. Depletion of A, C or U led to a slight decrease in membrane binding, whereas
177 removal of G showed a significant binding decrease. The decrease in binding affinity in all of the base-
178 depleted oligos (**Fig. 4b**) indicates that base-pairing may influence membrane binding. However, the
179 larger effect of G depletion indicates that either depletion of G causes highest bias on RNA base-pairing
180 or base pairing is not the only factor responsible for membrane binding, consistent with our previous
181 observation that G-content alone can influence binding (**Fig. 4a**). Finally, by comparing 19-mer and 40-

182 mer randomized oligos, we observed that increasing RNA length also led to enhanced binding, possibly
183 due to increased length and G content (**Fig. 4 a,b**).
184
185 To further determine how guanine content affects membrane binding, lipid-buffer partition
186 coefficients were determined for short oligomers with varying G-content. RNA membrane-buffer
187 partition coefficients indicate how well a particular molecule binds to the membrane by comparing the
188 relative amount of RNA in buffer and on the lipid membrane. The RNA oligos measured in this study
189 had partition coefficients around 10^5, which is in the range of partition coefficients determined for
190 hydrophobic peptides[49]. Remarkably, addition of 2 G's per oligo led to a 2.7-fold increase of the
191 partition coefficient relative to guanine-depleted RNA. Oligos with 4 and more guanine residues
192 showed a further increase of partition coefficient values with highest value for 9 G's. This result shows
193 that the presence of guanine affects RNA-lipid binding and even low guanine content significantly
194 increases membrane binding efficiency (**Fig. 4c**).
195
196 **RNA-membrane binding is dependent on RNA base pairing**
197 Our observations of the effect of base depletion on oligomer binding suggested that base-pairing may
198 be a key factor in membrane binding. To investigate the effect of base-pairing on membrane
199 interactions, we estimated binding efficiency for ssRNA and dsRNA (composed of 100%
200 complementary sequences) species. We observed that not only was the membrane binding efficiency
201 higher for dsRNA compared with ssRNA species, but also that only dsRNA promoted vesicle
202 aggregation (**Fig. 5a**). It is interesting to note that the difference in binding efficiency of the two ssRNAs,
203 which have identical base composition but different sequence, is consistent with the importance of
204 sequence as a key determinant of membrane binding. We further observed that dsRNA interacts with
205 fewer lipids than ssRNA, implying different models of binding (**Fig. 5b**). Thus, membrane binding
206 efficiency can be dependent on the propensity of an RNA molecule to form intra- or inter-molecular
207 structures through base pairing. Since base pairing is a fundamental element of RNA secondary
208 structure, our results indicate that structure in general can influence the selectivity of RNA-lipid
209 interactions.
210
211 To gain further insight into the effect of base pairing-dependent intra- and inter-molecular
212 interactions, we estimated the lipid-to-nucleotide binding ratios of ssRNA and dsRNA (**Fig. 5c**). By
213 calculating the molecular ratio of lipid/nucleotide binding, we introduce a normalization factor that
214 allows us to directly compare membrane binding for oligos of varying length. Furthermore, varying
215 lipid to nucleotide stoichiometry reflects changes in the average lipid/nucleotide interaction strength.
216 With this estimate, we compared lipid/nucleotide binding for ssRNA and dsRNA alongside oligos with
217 varying guanine content from our previous analysis (**Fig. 4c**)**.** The differences between ssRNA and
218 dsRNA, all containing 9 guanines per oligo, confirmed our previous observation that sequence variation
219 (with constant base content) and base pairing can both influence binding. However, the reason for a
220 change in lipid/nucleotide ratio for oligos with varying guanine content was not readily apparent.
221 Analysis of oligos with varying guanine content by native non-denaturing gel revealed that the
222 presence of guanine promotes a larger spread in migration (**Fig. 5c, inset**), indicating that guanines
223 promote intermolecular interactions. These observations show that guanine can enhance binding by
224 promoting intermolecular interactions, and further confirm the importance of base pairing in RNA-
225 lipid interactions.
226
227 **Modifying R3C substrate sequence enhances membrane binding and modifies reaction rates**

228 In previous experiments, we observed that the binding affinity of the short substrate was >3 orders of
229 magnitude lower than for the R3C ligase and that reaction rates correlated strongly with R3C-
230 membrane binding (**Fig. 3c, d**). We therefore reasoned that by modifying the R3C ligase substrate to
231 enhance membrane binding, we might be able to further modulate ligase activity through increased
232 RNA density at the membrane surface. Having determined that guanine content is a key factor
233 influencing RNA-lipid binding (**Fig. 4**), we modified the R3C substrate sequence to increase lipid
234 membrane binding efficiency by addition of a 5'-overhang with varying amounts of AG repeats (**Fig.
235 6a**).
236
237 We first assessed the effect of modifying the R3C ligase substrate on ligation rate in the absence of
238 membranes (**Fig. 6a**). We observed that increasing the guanine content decreased ligase activity,
239 suggesting that 5' modification of the substrate was inhibiting the reaction either through steric
240 hindrance or promotion of inhibitory inter- or intra-molecular interactions. To determine whether AG-
241 rich substrates form intra-molecular structures[50] or exhibit reduced binding with the R3C ligase, we
242 performed electrophoresis in native conditions with and without ligase (**Fig. 6b**). Firstly, the non-
243 modified short substrate migrated as one band and was fully bound to the R3C ligase. Secondly, a
244 4x(AG) 20 nt substrate variant migrated as two bands, which suggests that part of the substrate
245 molecules have some folding that might bias binding to the R3C ligase. In the presence of ligase, 30%
246 of the substrate was non-bound, which correlated with a 22% reduction in reaction rate. For the
247 longest substrate variant (31 nt), electrophoretic mobility suggested higher folding, since only one
248 band was present and migrated half-way between the non-folded 12 nt and 20 nt substrates. 70% of
249 the 9x(AG) substrate was not bound to the ligase, which correlates with a reduced R3C reaction rate.
250 Lastly, the AG-rich oligomer did not co-migrate with the R3C ligase, indicating that the inhibition effect
251 is not based on non-specific substrate-ligase interactions (not shown). Therefore, increasing guanine
252 content reduces R3C ligase-substrate binding, likely accounting for decreased activity.
253
254 We next investigated whether varying guanine content through 5' modification of the substrate
255 influences membrane binding and, consequently, ligation activity in the presence of membranes. As
256 expected, the longer guanine-containing R3C substrates showed significantly higher membrane
257 binding compared with the shorter variant (**Fig. 6c**). To determine whether binding of the substrates
258 to the membrane enhances ligase activity, we determined R3C reaction rates in the presence of the
259 gel lipid membranes (**Fig. 6d**). For modified substrates, the reaction rates increased significantly to the
260 level of the unmodified substrate. Interestingly, none of the modified substrates exhibited higher
261 activity than the unmodified substrate, indicating that the rescue of activity of the other guanine
262 variants is not due to increased substrate-ligase interactions through enhanced binding to the
263 membrane, but rather due to interaction of the membrane with 5' overhangs. Thus, substrate-
264 membrane interaction increases activity by rescuing the inhibitory effect of the guanine-rich 5'
265 overhangs (**Fig. 6e**).
266
267 In summary, by modifying the R3C ribozyme substrate with an additional short sequence containing
268 guanine residues, we increased membrane affinity. The addition of guanines, however, also introduced
269 an inhibitory effect on ligation activity that was reversed through the introduction of gel-membranes
270 to the reaction. Thus, we unexpectedly produced a lipid-sensitive riboswitch-like system that could be
271 tuned in a lipid concentration-dependent manner.
272
273 **Discussion**

We have demonstrated that RNA-gel membrane interactions are dependent on the nucleotide content and base pairing of ribonucleic acids. Varying the guanosine content of RNAs changed membrane-buffer partitioning by several orders of magnitude. Additionally, double-stranded RNAs exhibited higher membrane partitioning than single-stranded RNAs, indicating that secondary structure is a critical factor in RNA-membrane interactions. Although gel-membranes are not widely observed in living cells, RNA-gel membrane interactions could be employed for ribo-regulation in synthetic biological systems. Gel membranes also plausibly accumulated in ancient prebiotic scenarios, potentially serving as an organizational scaffold, as has been proposed for "ribofilms" on mineral surfaces[51]. Furthermore, understanding the factors involved in RNA-gel membrane interactions should provide insights that can be used to design RNA sequences with affinity for physiologically relevant fluid membranes. Indeed, our finding that guanosine is a key factor in promoting RNA-gel membrane partitioning is consistent with previous speculation that guanosine residues might play a role in the binding of RNA aptamers to fluid membranes[38]. Taken together, the sequence and structural dependence of RNA-gel membrane interactions shown here provides the necessary framework to design synthetic RNAs with varying membrane affinities.

Our observation of riboswitch-like behavior suggests a novel mechanism for regulation of RNA through membrane interactions. Riboswitches are RNAs with regulatory effects that are derived from sensitivity to physicochemical conditions or through binding with an interaction partner. Riboswitch regulation through temperature changes, interaction with nucleic acids and small molecules have been described previously[52–56]. However, lipid sensitive riboswitches have not been documented. It is now plausible that spontaneously self-assembling lipid membranes in ancient environments could have served as an organizational scaffold regulating the activity of RNAs in a sequence- and structure-dependent manner. Furthermore, the importance of guanosine in membrane binding suggests a possible mechanism for its selection as one of the canonical nucleic acids. In extant organisms, synthetic or naturally occurring RNAs exhibiting sensitivity to lipids could potentially act as biosensors or riboswitches. By demonstrating that RNA-gel membrane interactions can induce riboswitch-like behaviors, we raise the possibility that such functionalities could be an ancient mechanism of ribo-regulation and may be present among the myriad uncharacterized small RNAs in modern cells.

RNA-membrane interactions provide a means to select RNAs by sequence and structure. For example, diverse RNA species can be segregated or co-localized based on their differential membrane affinities. Furthermore, selective RNA-membrane localization can be controlled by shifting the temperature above and below the membrane gel-liquid transition temperature, thereby turning on and off RNA-membrane binding. Such lipid-dependent sorting of RNAs could provide a mechanism to selectively control the concentration of reactants in primordial scenarios and in synthetic RNA-based systems. Selective RNA-membrane interactions would also influence the sequence space explored by evolving ribozymes. Ribozymes generated through natural or artificial selection in the presence of lipid membranes may, therefore, evolve enhanced or novel functions. The sequence and structural selectivity of RNAs for membranes can also be implemented in the design of novel RNA membrane biosensors. Looking forward, RNA-membrane interactions can provide tools for selective ribo-regulation in synthetic systems, development of membrane biosensors, and might facilitate the emergence of novel functions through artificial and natural evolution of ribozymes in the presence of membranes.

In conclusion, our findings reveal that lipids, which are present in every modern cell and were plausibly part of a prebiotic world[57–59], can interact with RNA and change its activity. These findings have significant applications in fields such as synthetic biology, where merging the selective affinities of aptamers with ribozyme activity (aptazymes) is currently a developing field[60–62]. Our results provide a foundation for exploring the basis of membrane-RNA interactions with physiologically relevant fluid membranes exhibited by synthetic aptamers[16,40,63] thereby providing new regulatory mechanisms in synthetic biology through the specific and anchor-free localization of RNA molecules within lipid compartments. Furthermore, insights from the present study can already be implemented in bioengineering applications such as in improving mRNA drug delivery mechanisms and introducing lipid sensitive ribo-regulation to synthetic ribozyme networks. Finally, the interaction between RNA and lipid membranes could have provided an evolutionary pressure in ancient times through selection for base composition or secondary structural features.

Acknowledgements:

We would like to thank Mario Mörl, Ilya Levental, Robert Ernst, Andre Nadler, Dora Tang, Grzegorz Chwastek, Michał Grzybek and Mike Thompson for helpful discussions and feedback. We would also like to thank Anatol Fritsch for home-made microscopy stage-top temperature-control device. This work was supported by the B CUBE of the TU Dresden, a Simons Foundation Fellowship (to J.S.), a German Federal Ministry of Education and Research BMBF grant (to J.S., project 03Z22EN12), and a VW Foundation ''Life'' grant (to J.S., project 93090).

The authors declare no conflict of interests.

References

1. Pace, N. R. & Marsh, T. L. RNA catalysis and the origin of life. *Origins Life Evol B* **16,** 97–116 (1985).

2. Gilbert, W. Origin of life: The RNA world. *Nature* **319,** 618–618 (1986).

3. Rich, A. On the problems of evolution and biochemical information transfer. *Horizons in biochemistry* 103–126 (1962).

4. Breaker, R. R. Engineered allosteric ribozymes as biosensor components. *Curr Opin Biotech* **13,** 31–39 (2002).

5. Wittmann, A. & Suess, B. Engineered riboswitches: Expanding researchers' toolbox with synthetic RNA regulators. *Febs Lett* **586,** 2076–2083 (2012).

6. Isaacs, F. J., Dwyer, D. J. & Collins, J. J. RNA synthetic biology. *Nat Biotechnol* **24,** 545–554 (2006).

7. Bartel, D. & Szostak, J. Isolation of new ribozymes from a large pool of random sequences. *Science* **261,** 1411–1418 (1993).

359 8. Ekland, E., Szostak, J. & Bartel, D. Structurally complex and highly active RNA ligases
360 derived from random RNA sequences. *Science* **269,** 364–370 (1995).

361 9. Robertson, M. P., Hesselberth, J. R. & Ellington, A. D. Optimization and optimality of a
362 short ribozyme ligase that joins non-Watson–Crick base pairings. *Rna* **7,** 513–523 (2001).

363 10. Rogers, J. & Joyce, G. F. The effect of cytidine on the structure and function of an RNA
364 ligase ribozyme. *Rna* **7,** 395–404 (2001).

365 11. Paul, N. & Joyce, G. F. A self-replicating ligase ribozyme. *Proc National Acad Sci* **99,**
366 12733–12740 (2002).

367 12. Lincoln, T. A. & Joyce, G. F. Self-Sustained Replication of an RNA Enzyme. *Science* **323,**
368 1229–1232 (2009).

369 13. Saragliadis, A., Krajewski, S. S., Rehm, C., Narberhaus, F. & Hartig, J. S. Thermozymes:
370 synthetic RNA thermometers based on ribozyme activity. *Rna Biol* **10,** 1009–1016 (2013).

371 14. Ferretti, A. C. & Joyce, G. F. Kinetic Properties of an RNA Enzyme That Undergoes Self-
372 Sustained Exponential Amplification. *Biochemistry-us* **52,** 1227–1235 (2013).

373 15. Lam, B. J. & Joyce, G. F. Autocatalytic aptazymes enable ligand-dependent exponential
374 amplification of RNA. *Nat Biotechnol* **27,** 288–292 (2009).

375 16. Janas, T., Janas, T. & Yarus, M. A membrane transporter for tryptophan composed of
376 RNA. *Rna* **10,** 1541–1549 (2004).

377 17. Pino, S., Ciciriello, F., Costanzo, G. & Mauro, E. D. Nonenzymatic RNA Ligation in Water*.
378 *J Biol Chem* **283,** 36494–36503 (2008).

379 18. Guerrier-Takada, C., Gardiner, K., Marsh, T., Pace, N. & Altman, S. The RNA moiety of
380 ribonuclease P is the catalytic subunit of the enzyme. *Cell* **35,** 849–857 (1983).

381 19. Anella, F. & Danelon, C. Prebiotic Factors Influencing the Activity of a Ligase Ribozyme.
382 *Life* **7,** 17 (2017).

383 20. Dai, X., Zhang, S. & Zaleta-Rivera, K. RNA: interactions drive functionalities. *Mol Biol Rep*
384 **47,** 1413–1434 (2020).

385 21. Müller, U. F. & Bartel, D. P. Improved polymerase ribozyme efficiency on hydrophobic
386 assemblies. *Rna* **14,** 552–562 (2008).

387 22. Anella, F. & Danelon, C. Reconciling Ligase Ribozyme Activity with Fatty Acid Vesicle
388 Stability. *Life* **4,** 929–943 (2014).

389 23. Chen, I. A., Salehi-Ashtiani, K. & Szostak, J. W. RNA Catalysis in Model Protocell Vesicles. *J*
390 *Am Chem Soc* **127,** 13213–13219 (2005).

391 24. Mansy, S. S., Schrum, J. P., Krishnamurthy, M., Tobé, S., Treco, D. A. & Szostak, J. W.
392 Template-directed synthesis of a genetic polymer in a model protocell. *Nature* **454,** 122–125
393 (2008).

394 25. Bianconi, G., Zhao, K., Chen, I. A. & Nowak, M. A. Selection for Replicases in Protocells.
395 *Plos Comput Biol* **9,** e1003051 (2013).

396 26. Budker, V. G., Kazatchkov, Yu. A. & Naumova, L. P. Polynucleotides adsorb on
397 mitochondrial and model lipid membranes in the presence of bivalent cations. *Febs Lett* **95,**
398 143–146 (1978).

399 27. McManus, J. J., Rädler, J. O. & Dawson, K. A. Does Calcium Turn a Zwitterionic Lipid
400 Cationic? *J Phys Chem B* **107,** 9869–9875 (2003).

401 28. Kharakoz, D. P., Khusainova, R. S., Gorelov, A. V. & Dawson, K. A. Stoichiometry of
402 dipalmitoylphosphatidylcholine-DNA interaction in the presence of Ca2+: a temperature-
403 scanning ultrasonic study. *Febs Lett* **446,** 27–29 (1999).

404 29. Gromelski, S. & Brezesinski, G. Adsorption of DNA to zwitterionic DMPE monolayers
405 mediated by magnesium ions. *Phys Chem Chem Phys* **6,** 5551–5556 (2004).

406 30. Uhríková, D., Hanulová, M., Funari, S. S., Khusainova, R. S., Šeršeň, F. & Balgavý, P. The
407 structure of DNA–DOPC aggregates formed in presence of calcium and magnesium ions: A
408 small-angle synchrotron X-ray diffraction study. *Biochimica Et Biophysica Acta Bba -*
409 *Biomembr* **1713,** 15–28 (2005).

410 31. Gromelski, S. & Brezesinski, G. DNA Condensation and Interaction with Zwitterionic
411 Phospholipids Mediated by Divalent Cations. *Langmuir* **22,** 6293–6301 (2006).

412 32. McLoughlin, D., Dias, R., Lindman, B., Cardenas, M., Nylander, T., Dawson, K., Miguel, M.
413 & Langevin, D. Surface Complexation of DNA with Insoluble Monolayers. Influence of
414 Divalent Counterions. *Langmuir* **21,** 1900–1907 (2005).

415 33. Michanek, A., Yanez, M., Wacklin, H., Hughes, A., Nylander, T. & Sparr, E. RNA and DNA
416 Association to Zwitterionic and Charged Monolayers at the Air–Liquid Interface. *Langmuir*
417 **28,** 9621–9633 (2012).

418 34. Michanek, A., Kristen, N., Höök, F., Nylander, T. & Sparr, E. RNA and DNA interactions
419 with zwitterionic and charged lipid membranes — A DSC and QCM-D study. *Biochimica Et*
420 *Biophysica Acta Bba - Biomembr* **1798,** 829–838 (2010).

421 35. Marty, R., N'soukpoé-Kossi, C. N., Charbonneau, D. M., Kreplak, L. & Tajmir-Riahi, H.-A.
422 Structural characterization of cationic lipid–tRNA complexes. *Nucleic Acids Res* **37,** 5197–
423 5207 (2009).

424 36. Suga, K., Tanabe, T., Tomita, H., Shimanouchi, T. & Umakoshi, H. Conformational change
425 of single-stranded RNAs induced by liposome binding. *Nucleic Acids Res* **39,** 8891–8900
426 (2011).

427 37. Lu, D. & Rhodes, D. G. Binding of phosphorothioate oligonucleotides to zwitterionic
428 liposomes. *Biochimica Et Biophysica Acta Bba - Biomembr* **1563,** 45–52 (2002).

429 38. Khvorova, A., Kwak, Y.-G., Tamkun, M., Majerfeld, I. & Yarus, M. RNAs that bind and
430 change the permeability of phospholipid membranes. *Proc National Acad Sci* **96,** 10649–
431 10654 (1999).

432 39. Vlassov, A. & Yarus, M. Interaction of RNA with Phospholipid Membranes. *Mol Biol+* **36,**
433 389–393 (2002).

434 40. Vlassov, A., Khvorova, A. & Yarus, M. Binding and disruption of phospholipid bilayers by
435 supramolecular RNA complexes. *Proc National Acad Sci* **98,** 7706–7711 (2001).

436 41. Janas, T., Janas, T. & Yarus, M. Specific RNA binding to ordered phospholipid bilayers.
437 *Nucleic Acids Res* **34,** 2128–2136 (2006).

438 42. Pannwitt, S., Slama, K., Depoix, F., Helm, M. & Schneider, D. Against Expectations:
439 Unassisted RNA Adsorption onto Negatively Charged Lipid Bilayers. *Langmuir* **35,** 14704–
440 14711 (2019).

441 43. Kruger, K., Grabowski, P. J., Zaug, A. J., Sands, J., Gottschling, D. E. & Cech, T. R. Self-
442 splicing RNA: Autoexcision and autocyclization of the ribosomal RNA intervening sequence
443 of tetrahymena. *Cell* **31,** 147–157 (1982).

444 44. Quarless, S. A. & Cantor, C. R. Analysis of RNA structure by ultraviolet crosslinking and
445 denaturation gel electrophoresis. *Anal Biochem* **147,** 296–300 (1985).

446 45. Behlen, L. S., Sampson, J. R. & Uhlenbeck, O. C. An ultraviolet light-induced crosslink in
447 yeast tRNA phe. *Nucleic Acids Res* **20,** 4055–4059 (1992).

448 46. Nejedlý, K., Kittner, R., Pospíšilová, Š. & Kypr, J. Crosslinking of the complementary
449 strands of DNA by UV light: dependence on the oligonucleotide composition of the UV
450 irradiated DNA. *Biochimica Et Biophysica Acta Bba - Gene Struct Expr* **1517,** 365–375 (2001).

451 47. Lengyel, A., Uhríková, D., Klacsová, M. & Balgavý, P. DNA condensation and its thermal
452 stability influenced by phospholipid bilayer and divalent cations. *Colloids Surfaces B*
453 *Biointerfaces* **86,** 212–217 (2011).

454 48. Black, R. A., Blosser, M. C., Stottrup, B. L., Tavakley, R., Deamer, D. W. & Keller, S. L.
455 Nucleobases bind to and stabilize aggregates of a prebiotic amphiphile, providing a viable
456 mechanism for the emergence of protocells. *Proc National Acad Sci* **110,** 13272–13276
457 (2013).

458 49. White, S. H., Wimley, W. C., Ladokhin, A. S. & Hristova, K. [4] Protein folding in
459 membranes: Determining energetics of peptide-bilayer interactions. *Methods Enzymol* **295,**
460 62–87 (1998).

461 50. Lee, J. S., Evans, D. H. & Morgan, A. R. Polypurine DNAs and RNAs form secondary
462 structures which may be tetra-stranded. *Nucleic Acids Res* **8,** 4305–4320 (1980).

463 51. Baross, J. A. & Martin, W. F. The Ribofilm as a Concept for Life's Origins. *Cell* **162,** 13–15
464 (2015).

465 52. Johansson, J., Mandin, P., Renzoni, A., Chiaruttini, C., Springer, M. & Cossart, P. An RNA
466 Thermosensor Controls Expression of Virulence Genes in Listeria monocytogenes. *Cell* **110,**
467 551–561 (2002).

468 53. Winkler, W., Nahvi, A. & Breaker, R. R. Thiamine derivatives bind messenger RNAs
469 directly to regulate bacterial gene expression. *Nature* **419,** 952–956 (2002).

470 54. Morita, M. T., Tanaka, Y., Kodama, T. S., Kyogoku, Y., Yanagi, H. & Yura, T. Translational
471 induction of heat shock transcription factor ς32: evidence for a built-in RNA thermosensor.
472 *Gene Dev* **13,** 655–665 (1999).

473 55. Schilling, O., Langbein, I., Müller, M., Schmalisch, M. H. & Stülke, J. A protein-dependent
474 riboswitch controlling ptsGHI operon expression in Bacillus subtilis: RNA structure rather
475 than sequence provides interaction specificity. *Nucleic Acids Res* **32,** 2853–2864 (2004).

476 56. Nahvi, A., Sudarsan, N., Ebert, M. S., Zou, X., Brown, K. L. & Breaker, R. R. Genetic Control
477 by a Metabolite Binding mRNA. *Chem Biol* **9,** 1043–1049 (2002).

478 57. Patel, B. H., Percivalle, C., Ritson, D. J., Duffy, C. D. & Sutherland, J. D. Common origins of
479 RNA, protein and lipid precursors in a cyanosulfidic protometabolism. *Nat Chem* **7,** 301–307
480 (2015).

481 58. Rushdi, A. I. & Simoneit, B. R. T. Lipid Formation by Aqueous Fischer-Tropsch-Type
482 Synthesis over a Temperature Range of 100 to 400 °C. *Origins Life Evol B* **31,** 103–118 (2001).

483 59. Brady, R. C. & Pettit, R. Mechanism of the Fischer-Tropsch reaction. The chain
484 propagation step. *J Am Chem Soc* **103,** 1287–1289 (1981).

485 60. Robertson, M. P. & Ellington, A. D. Design and optimization of effector-activated
486 ribozyme ligases. *Nucleic Acids Res* **28,** 1751–1759 (2000).

487 61. Debiais, M., Lelievre, A., Smietana, M. & Müller, S. Splitting aptamers and nucleic acid
488 enzymes for the development of advanced biosensors. *Nucleic Acids Res* **48,** 3400–3422
489 (2020).

490 62. Stifel, J., Spöring, M. & Hartig, J. S. Expanding the toolbox of synthetic riboswitches with
491 guanine-dependent aptazymes. *Synthetic Biology* **4,** ysy022- (2019).

492 63. Janas, T. & Yarus, M. Visualization of membrane RNAs. *Rna* **9,** 1353–1361 (2003).

493 64. Walker, S. C., Avis, J. M. & Conn, G. L. General plasmids for producing RNA in vitro
494 transcripts with homogeneous ends. *Nucleic Acids Res* **31,** e82–e82 (2003).

495 65. Schmidt, M. L., Ziani, L., Boudreau, M. & Davis, J. H. Phase equilibria in DOPC/DPPC:
496 Conversion from gel to subgel in two component mixtures. *J Chem Phys* **131,** 175103 (2009).

497 66. Schindelin, J., Arganda-Carreras, I., Frise, E., Kaynig, V., Longair, M., Pietzsch, T.,
498 Preibisch, S., Rueden, C., Saalfeld, S., Schmid, B., Tinevez, J.-Y., White, D. J., Hartenstein, V.,
499 Eliceiri, K., Tomancak, P. & Cardona, A. Fiji: an open-source platform for biological-image
500 analysis. *Nat Methods* **9,** 676–682 (2012).

501 67. Chen, P. S., Toribara, T. Y. & Warner, H. Microdetermination of Phosphorus. *Anal Chem*
502 **28,** 1756–1758 (1956).

503
504
505
506
507

508 ## Materials and methods

509 **Materials**

510 Dipalmitoylphosphatidylcholine (DPPC), dioleoylphosphatidylcholine (DOPC) and biotinylated
511 phosphatidylethanolamine (18:1 biotinyl cap PE) were purchased from Avanti Polar Lipids (USA) and
512 were used without further purification. HEPES, $MgCl_2$ and $CaCl_2$ were purchased from CarlRoth
513 (Germany) and were at least >99% pure. All solutions were prepared in MilliQ water, Merck Millipore
514 (USA).
515
516 The R3C ligase construct[10] was cloned into the pRZ plasmid[64] using the InFusion cloning system (Takara
517 Bio, Japan). To ensure correct length of transcript, pRZ-R3C plasmid was treated with EcoRI-HF (NEB,
518 USA). RNA wasexpressed using T7 RNA polymerase (homemade, MPI-CBG, Germany) at 37 °C
519 overnight, followed by 10 cycles of 5' 60 °C -> 5' 24 °C (HDV cleavage of construct to release pure R3C)
520 and DNAse I treatment (Thermo Scientific, USA). 75-85 randomised oligomer was expressed using
521 artificial DNA template (Eurofins Genomics, Germany) – both R3C and randomer were purified using
522 phenol-chloroform-isoamyl alcohol extraction, denaturing PAGE and electroelution. 5' 6-FAM labelled
523 R3C substrates as well as other short oligomers used in binding assays were obtained from Integrated
524 DNA Technologies (USA) and used without further purification.

Sequence name	**Sequence (5' – 3')**
R3C	GAGACCGUAAUGAGUAGUACUUAUUAUGCUCGAUUGUUCGUAAG AACAGUUUGAAUGGGUUGAAUAUAGUGAGGAUCCGCUAGC
Short substrate	6_FAM_CGACUCACUAUA
4xAG substrate	6_FAM_A**G**A**G**A**G**A**G**CGACUCACUAUA
9xAG substrate	6_FAM_A**G**A**G**A**G**A**G**A**G**A**G**A**G**A**G**A**G**ACGACUCACUAUA
2G substrate	6_FAM_HHHHHHHH**G**HHH**G**HHHHHHCGACUCACUAUA
0G	HHHHHHHHHHHHHHHHHHHHHHHHHHHHHHHHHHHH
2G	HHHHHHHHHHHHHHHH**G**HHH**G**HHHHHHHHHHHHHHHHH
4G	HHHHHHHHHHHH**G**HHH**G**HHH**G**HHH**G**HHHHHHHHHHH
5G	HHHHHHHHHH**G**HHH**G**HHH**G**HHH**G**HHH**G**HHHHHHHHHH
7G	HHHHHH**G**HHH**G**HHH**G**HHH**G**HHH**G**HHH**G**HHH**G**HHHHHH
9G	HH**G**HHH**G**HHH**G**HHH**G**HHH**G**HHH**G**HHH**G**HHH**G**HH

40xN	NNNNNNNNNNNNNNNNNNNNNNNNNNNNNNNNNNNNNNNN
40xN - G	HHHHHHHHHHHHHHHHHHHHHHHHHHHHHHHHHHHHHHHH
40xN - A	BBBBBBBBBBBBBBBBBBBBBBBBBBBBBBBBBBBBBBBB
40xN - C	DDDDDDDDDDDDDDDDDDDDDDDDDDDDDDDDDDDDDDDD
40xN - U	VVVVVVVVVVVVVVVVVVVVVVVVVVVVVVVVVVVVVVVV
19xG	**GGGGGGGGGGGGGGGGGGG**
19xA	AAAAAAAAAAAAAAAAAAA
19xC	CCCCCCCCCCCCCCCCCCC
19xU	UUUUUUUUUUUUUUUUUUU
19xN	NNNNNNNNNNNNNNNNNNN
AG repeats	6_FAM_AGAGAGAGAGAGAGAGAGA
ssRNA (ACUG)	ACUGACUGACUGACUGACUGACUGACUGACUGACUG
ssRNA (CAGU)	CAGUCAGUCAGUCAGUCAGUCAGUCAGUCAGUCAGU

B – C, G or U
D – A, G or U
H – A, C or U
V – A, C or G

Methods

All of the RNA incubations were prepared in DNA low bind tubes (Sarstedt, Germany) at the constant temperature of 24 °C in buffer comprised of 10 mM HEPES pH 7, 5 mM $CaCl_2$, and 5 mM $MgCl_2$. RNA concentration was determined by measuring absorbance at 260 nm (SPARK 20M, TECAN). Before every incubation RNA was preheated in SafeLock tubes (90 °C, 5 minutes; Eppendorf, Germany) to ensure unfolded structures. Denaturing PAGE analysis was performed using 10% 19:1 acrylamide:bisacrylamide gel composition, whereas native gels were composed of 8-10% 20:1 acrylamide:bisacrylamide mix. Before application on the denaturing PAGE all of the samples were ethanol precipitated.

Structure of R3C ligase from Fig. 2d was generated using RNA structure Fold tool from Mathews lab (https://rna.urmc.rochester.edu/RNAstructureWeb/).

Giant unilamellar vesicle (GUV) preparation and microscopy imaging

Gel-liquid phase separated vesicles were prepared from mixtures of DOPC:DPPC in a 1:1 molar ratio[65] with 0.5 mol% DiD (Invitrogen, USA). 20 nmol of total lipids were evenly distributed on Pt electrodes and dried under the vacuum for 15 minutes. Electroformation (10 Hz, 2.5 V, 65 °C) was conducted in 1 mM HEPES pH 7 and 300 mM sucrose for 3 hours followed by 30' of lower frequency current to promote GUVs formation (2 Hz, 2.5 V, 30').

GUVs were visualized in a home-made microscopy chamber with temperature control in isosmotic solution of glucose and buffer (260 mM glucose, 10 mM HEPES pH 7, 5 mM $MgCl_2$ and 5 mM $CaCl_2$). A Leica DMi8 confocal microscope coupled with a camera (Leica DFC9000 GTC) was used for image acquisition. For both confocal as well as camera acquisition 63x water-immersed objective was used.

556 For the confocal image acquisition, 488 nm (SybrGold) and 635 nm (DiD) lasers were used at low power
557 (<0.5%) to avoid photobleaching and the signal was collected using hybrid detectors (500 - 550 nm for
558 SybrGold and 700 – 800 nm for DiD). Z-scans were acquired as 6-8 averaged images per layer and Z-
559 stacked as a sum of the slides using FIJI software[66].
560
561 Temperature ramps were captured using a camera with FITC dichroicsfdichroics for DiD detection. 1.5
562 sec of exposure without binning was used to acquire each channel and measurement was repeated
563 every 5 seconds. Temperature changes were registered and calculated to be 3.4 °C/min. Image analysis
564 was conducted in FIJI software.
565
566 **Small lipid vesicle preparation**
567 DPPC chloroform stock was pipetted into a glass vial and briefly evaporated under a steady flow of
568 nitrogen gas. To remove organic solvent residues, a lipid film was dried under vacuum overnight. To
569 obtain multi-layer DPPC vesicles (MLV DPPC), lipid films were hydrated in reaction buffer, with a final
570 lipid concentration of 10 mM in 1 mL. Buffer-lipid mixtures were shaken at 60 °C, above the melting
571 temperature of DPPC (T_m = 42 °C), for one hour. A cloudy liposome suspension was freeze-and-thawed
572 10x and extruded 17x through 100 nm polycarbonate filters (Merck Millipore, USA) to reduce multi-
573 lamellarity and achieve a consistent size distribution of vesicles. Lipid vesicle stocks were kept at 4 °C.
574 Stock lipid concentrations were confirmed using a phosphate assay[67].
575
576 **Dynamic light scattering**
577 The size distribution of DPPC vesicles was estimated using a ZetaSizer Nano in 173° backscatter with
578 multiple narrow mode (high resolution) analysis. Final concentration of lipids was 10 μM and the
579 amount of RNA was fixed at a ratio of 10 lipids / nucleotide. Results were plotted as the size distribution
580 in the number of detected species (NumberPSD).
581
582 **UV-crosslinking**
583 RNA was incubated for 10 minutes in the reaction buffer with or without lipids followed by 10 minutes
584 incubation under UV-B light (300 mW LEUVA77N50KKU00 LED 305 nm) from a distance of 1.5 – 2 cm.
585 Samples were analysed on denaturing PAGE with SybrGold poststaining.
586
587 **R3C activity assays**
588 5 pmol of R3C ligase was mixed with 0.5 pmol of the substrate to ensure saturation of the system
589 (pseudo 1st order reaction) and decrease any batch-to-batch differences coming from R3C purification.
590 Final reaction volume was adjusted to 30 μl. Incubation was conducted at various concentrations of
591 DPPC vesicles and samples were ethanol precipitated after 30, 60, 90 and 120 minutes. Reactions were
592 quantified on denaturing PAGE using FIJI software. Product and substrate intensities (I_P and I_S,
593 respectively) were quantified and the concentration of product at time t was calculated:
594
595 $$[\boldsymbol{P}]_{\boldsymbol{t}} = [\boldsymbol{S}]_{\mathbf{0}} * \left(\frac{\boldsymbol{I_P}}{\boldsymbol{I_P} + \boldsymbol{I_S}}\right)$$
596
597 To determine reaction rates (M/min), concentration of the product was plotted as a function of time
598 and then fitted with a linear function (fixed [0;0] point).
599
600 **RNA-lipid binding assays**

601 Binding assays for the results in Fig. 3c (R3C ligase), Fig. 4a, b, c and Fig. 5a were conducted using
602 liposome-coated magnetic beads. Binding assays for the results in Fig. 2b, c and 5b, c were conducted
603 using an ultracentrifugation method.
604
605 **Magnetic beads binding assay**
606 Magnetic beads (DynaBeads streptavidin T1, Invitrogen) were coupled with DPPC liposomes doped
607 with 0.5 mol% biotynoyl cap PE. Lipid concentration on non-diluted beads was estimated using a
608 phosphate assay[67]. Liposome conjugated beads final working concentration was of 800 μM lipid.
609
610 25 pmol of 19 nt or 10 pmol of 40/36 nt RNAs were incubated with 2 – 1.5x diluted magnetic beads for
611 30'. After incubation the supernatant was separated from the beads using a magnet. The amount of
612 RNA left in solution was estimated either using absorbance or Qubit miRNA quantification kit
613 (ThermoScientific, USA). The reported binding efficiencies (Fig. 4a, b) correspond to 15 μL of liposome-
614 coated beads in a 30 μL reaction volume. The partition coefficient K (Fig. 4c, Fig. 5a) was calculated
615 according to following formula:
616
617
618
619
620

$$K = \frac{\frac{[R_L]}{[R_L] + [L]}}{\frac{[R_w]}{[R_w] + [W]}} \qquad \text{Eq. 1}$$

621
622 **Assuming high excess of [L] and [W] we simplified the equation to:**
623
624
625
626
627

$$K = \frac{\frac{[R_L]}{[L]}}{\frac{[R_w]}{[W]}} \qquad \text{Eq. 2}$$

628 **Where:**
629 **[R_L] – RNA bound to the membranes**
630 **[R_W] – non-bound RNA**
631 **[L] – outer lipid concentration**
632 **[W] – water concentration**
633
634
635 **Ultracentrifugation binding assay**
636 RNA was incubated with various concentrations of DPPC vesicles for 30'. After incubation
637 ultracentrifugation was conducted to separate vesicles from the solution (125 000 x G, 40', 24 °C). 9
638 μL of supernatant (out of 30 μL reaction mix) was pulled and incubated with 1.5 μL of 0.5 M EDTA (90
639 °C, 5'). After incubation 150 μl of 1xQubit dye was added to the solution and the amount of RNA was
640 measured using a plate reader (SPARK 20M, TECAN).
641
642 Measured fluorescence intensity values were plotted as a function of lipid/oligomer or lipid/nucleotide
643 ratios (we assumed that RNA interacts only with the outer membrane leaflet, so final outer lipid
644 concentration is equal half of the total lipid amount) and fitted using Hill's fit (OriginLab software):
645

Eq. 3

646 $$f(x) = Start + (End - Start)\frac{x^n}{x^n + k^n}$$

647

648 Where Start and End are function plateau values, k is inflection point of curve and n is cooperativity
649 index. Inflection point of the curve (k) is a parameter which we used for further data analysis.

650

651 **RNA-lipid binding partition coefficient determination for R3C substrates**

652 5 pmol of RNA was incubated with an excess of DPPC vesicles (5 mM, 2.5 mM outer leaflet) for 30
653 minutes. After incubation ultracentrifugation was conducted to separate vesicles from solution (125
654 000 x G, 40', 24 °C). 10 μL out of 30 μL was taken as a supernatant sample, and the rest of the
655 supernatant was discarded to leave only the pellet. RNA from supernatant and pellet samples was
656 ethanol precipitated and analyzed using denaturing PAGE. Partition coefficient values (Fig. 3c
657 "substrate", Fig. 6c) were calculated using Eq. 2.

658

659 **Statistical analysis**

660 All of the binding efficiency, partition coefficient, crosslinking efficiency and R3C activity assays were
661 repeated at least 3 times. Presented error bars are SEM values. Fits to the lipid/RNA binding assay ratio
662 determinations were included with $R^2 > 0.9$.

663

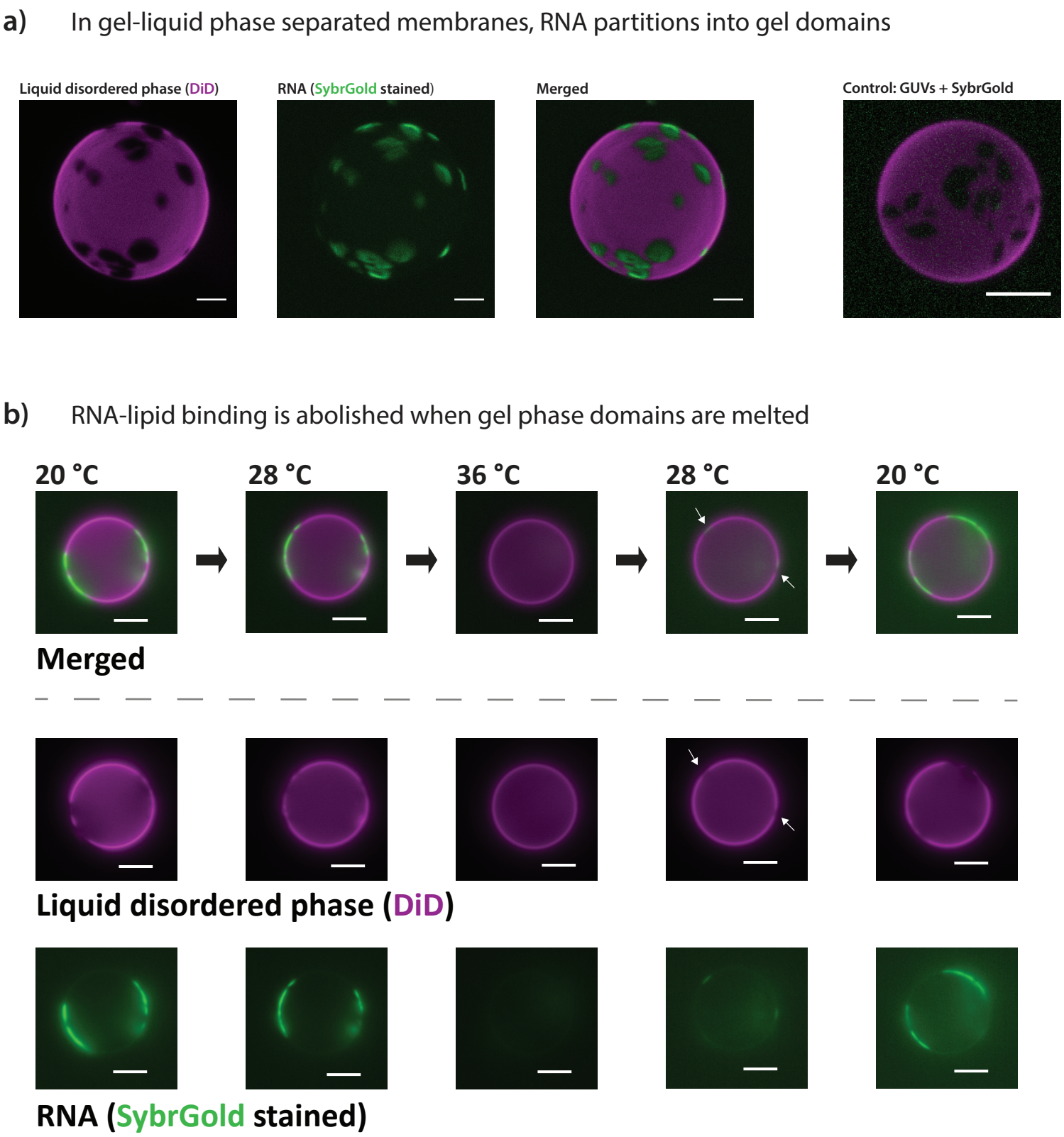

Fig. 1 RNA selectively binds to gel phase membrane domains. (a) gel-liquid phase separated giant unilamellar vesicles (GUVs) were prepared from a mixture of DOPC and DPPC with a molar ratio of 1:1 and labeled with 0.5 mol % of the fluorescent lipophilic probe DiD. DiD is excluded from gel phase domains, which are observed as non-stained regions on the surface of the vesicle. A mixture of random RNA oligomers (40xN) stained with SybrGold is enriched within the gel phase domains. A control without RNA shows that SybrGold itself does not stain the GUVs. **(b)** When gel phase domains are melted by increasing temperature (3.4 °C/min – see supplementary movie 1) RNA no longer enriches at the GUV surface. Decreasing the temperature again restores gel-liquid phase separation and, consequently, RNA-membrane binding (~28 °C, white arrows – see supplementary movie 2). All of the scale bars are 5 μm.

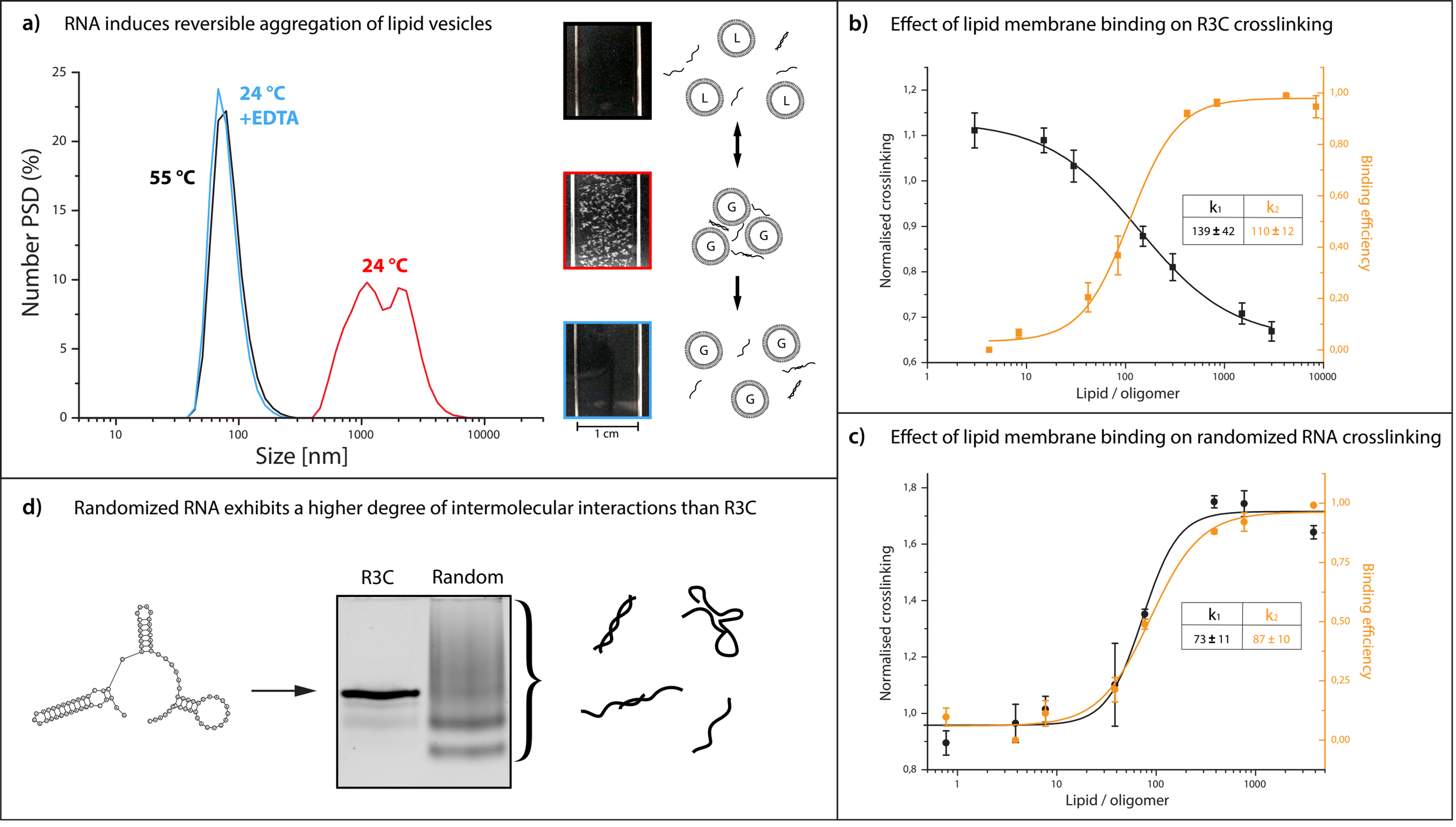

Fig. 2 RNA-lipid interactions induce reversible aggregation of vesicles and enhance intermolecular RNA interactions. (a) RNA-induced vesicular aggregation can be observed through changes in vesicle size distribution measured by dynamic light scattering (left), or visually as depicted in the cuvette images (right). The introduction of a randomized pool of RNA oligos to gel lipid membranes (gel phase = **G**) induces vesicle aggregation, which can be reversed either through chelation of divalent cations with EDTA or by increasing the temperature to achieve membranes in a liquid phase (liquid phase = **L**). **(b)** R3C ligase (84 nt) shows a small increase in UV-crosslinking at low lipid concentration, whereas crosslinking efficiency decreases at higher lipid concentration. Binding and UV crosslinking are inversely correlated and show similar inflection points with respect to lipid concentration. **(c)** Randomized RNA oligos (75-85 nt) show increasing crosslinking efficiency in the presence of lipids with a slight decrease at the highest lipid concentration; crosslinking and lipid binding are closely correlated. **(d)** Analysis of RNAs by native PAGE gel demonstrates that the R3C ligase forms primarily one structure, whereas randomized RNA forms diverse intermolecular complexes.

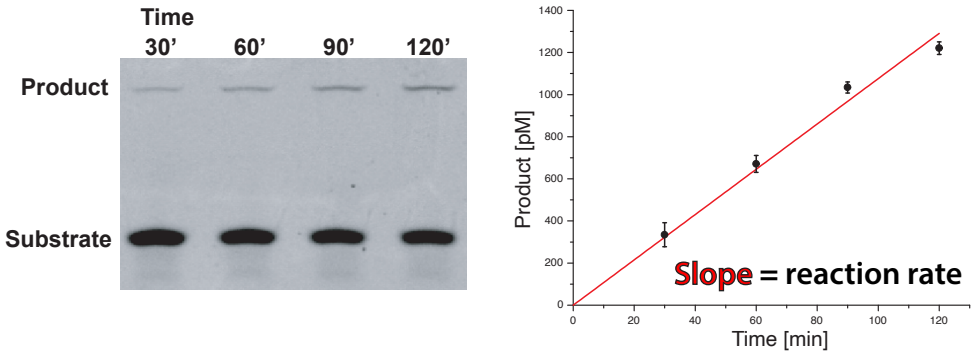

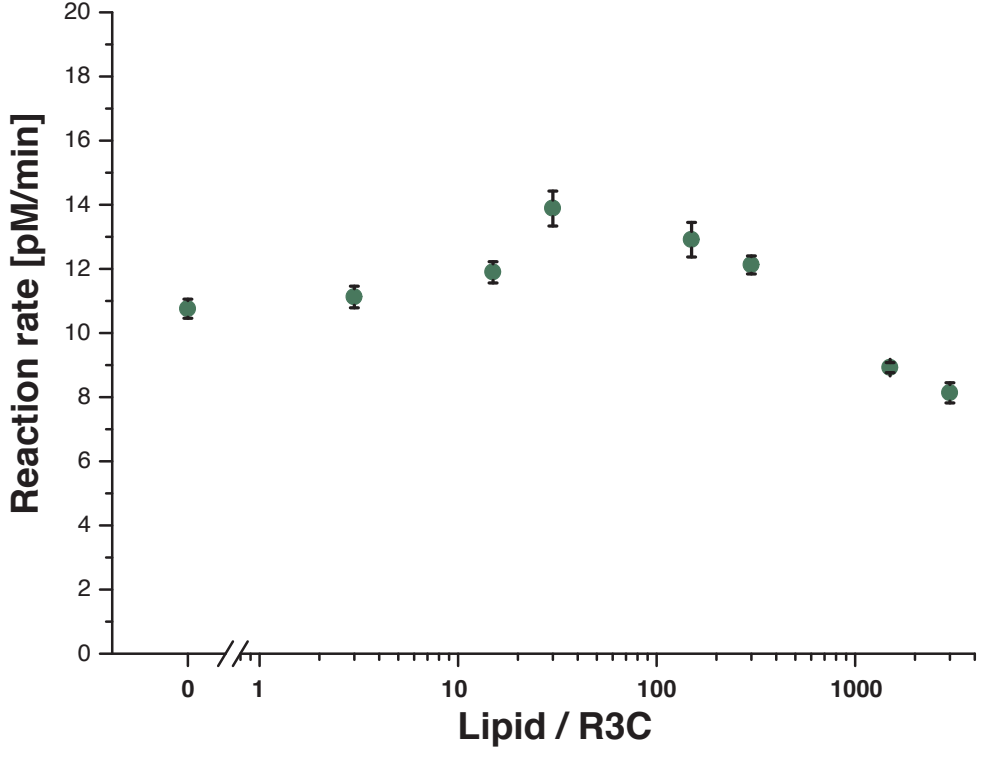

c) Lipid binding and nucleotide characteristics of R3C reactants

Oligo	log(K)	Nucleotide %				Length
		G	A	C	U	
R3C	**7.22 ±** 0.08	27	28	13	31	84 nt
Substrate	**3.39 ±** 0.15	8	33	33	25	12 nt

Fig. 3 Lipid membranes influence R3C ligase activity through lipid-ligase interactions. (a) R3C ligase reaction rates were quantified by measuring the amount of product within a 2 hour incubation time. **(b)** R3C reaction rate is dependent on the presence of gel membranes - increased activity is observed for lower lipid concentration followed by drop in activity at higher lipid concentration. **(c)** The 12 nt R3C substrate shows several orders of magnitude lower membrane-buffer partition coefficient log(K) compared with the R3C ligase, which could be derived from different compositional or structural characteristics of both RNA species.

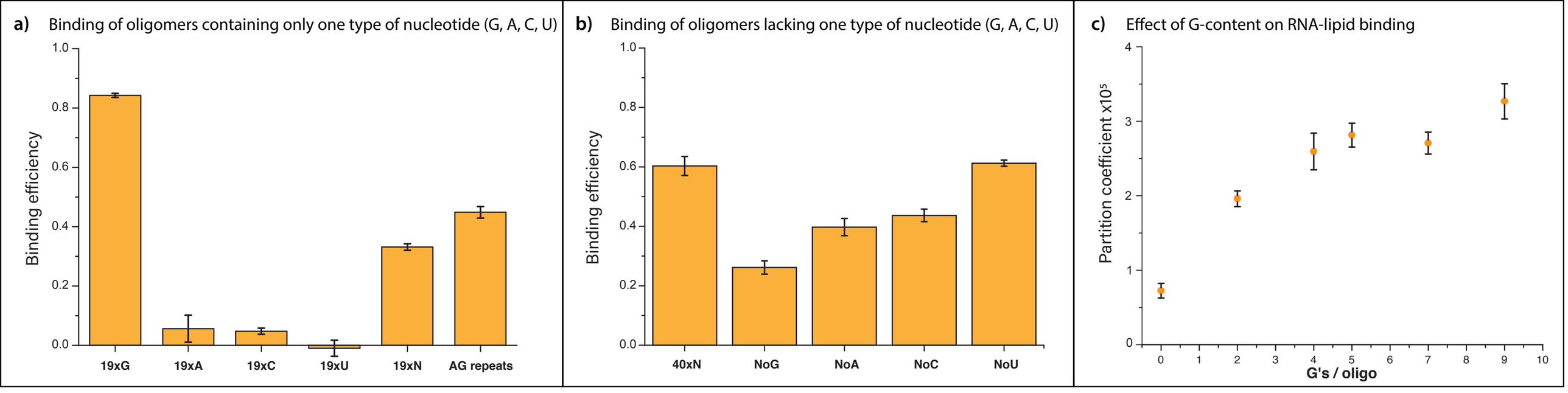

Fig. 4 RNA-lipid binding is RNA sequence-dependent. (a) Short 19 nucleotide oligomers show sequence-dependent binding to the gel membranes, with highest binding observed for the pure G oligomer followed by oligos with randomized sequence or AG repeats. Oligomers containing only A, C or U bases show negligible binding to the lipid membranes. **(b)** Oligonucleotide length also influences binding efficiency as seen in the comparison of **(a)** 19xN and **(b)** 40xN. Depletion of one type of nucleotide within oligomers lowers binding efficiency. Lack of guanine decreased binding by 57%, whereas lack of adenine, uracil or cytidine showed a less pronounced effect. **(c)** Oligonucleotides with increasing G content showed higher lipid – buffer partition coefficients compared to a G-deficient oligo with the highest value observed for the 9xG oligomer.

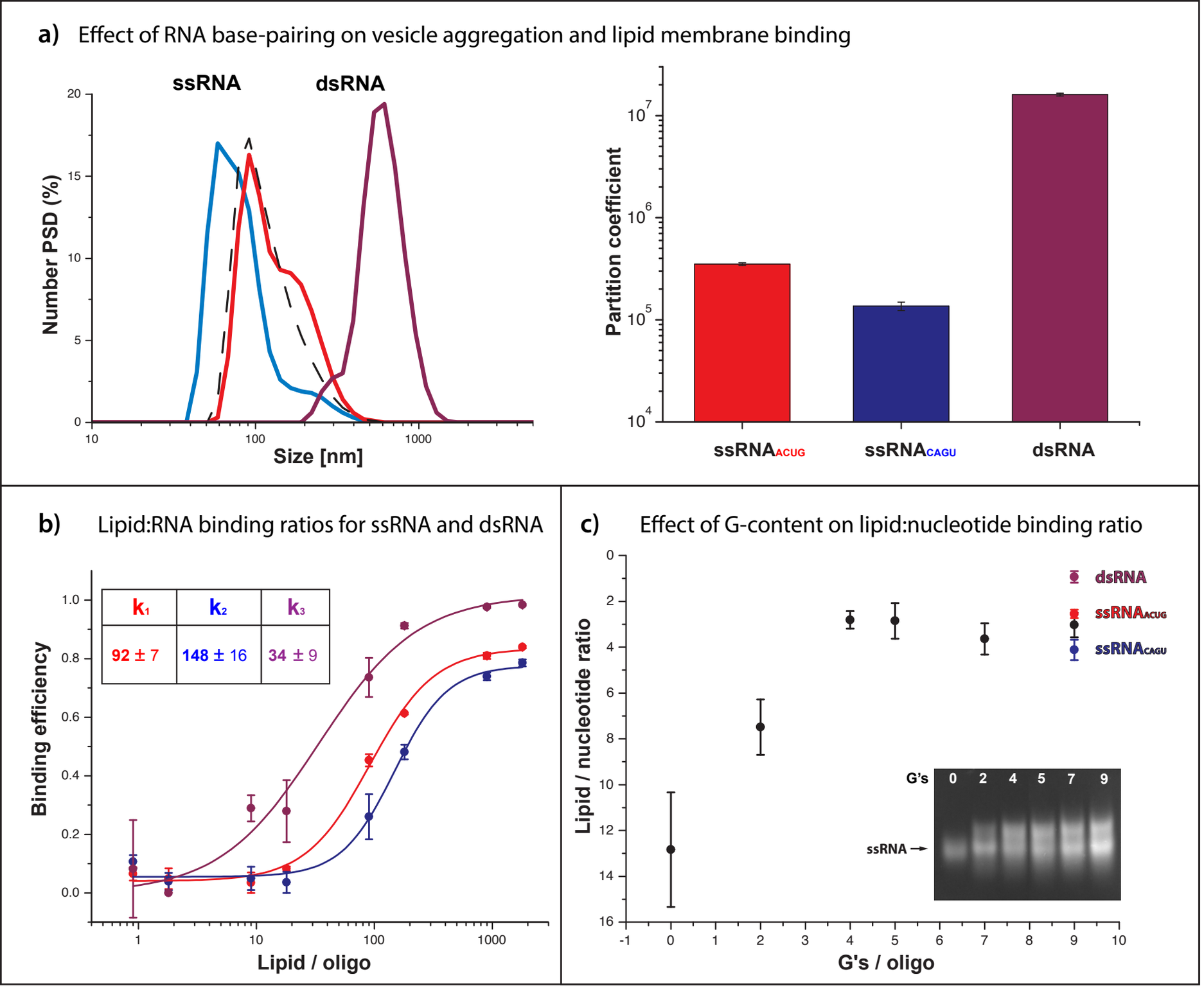

Fig. 5 RNA-gel membrane binding depends on RNA structure. (a) The effect of RNA base-pairing structure on lipid vesicle aggregation (left) and membrane binding (right) was evaluated by comparing RNA's with limited ability to create inter- and intramolecular structures (ssRNA: 36 nucleotide ACUG or CAGU repeats) with 100% complementary double stranded RNAs (dsRNA: mixed ACUG and CAGU oligos). Single stranded RNAs do not cause lipid vesicle aggregation despite moderate membrane binding, whereas double stranded RNA species show both high binding and vesicle aggregation. **(b)** RNA:lipid binding ratios (shown in table) estimated from binding curves of ssRNA and dsRNA (plotted) are affected by base pairing and sequence. **(c)** Oligomers with different nucleotide composition show different lipid/nucleotide binding stoichiometry. Analysis of oligomers by native PAGE gel **(c, inset)** indicates that the presence of guanine promotes inter-molecular interactions, suggesting, that base-pairing enhances the average strength of nucleotide-lipid interactions.

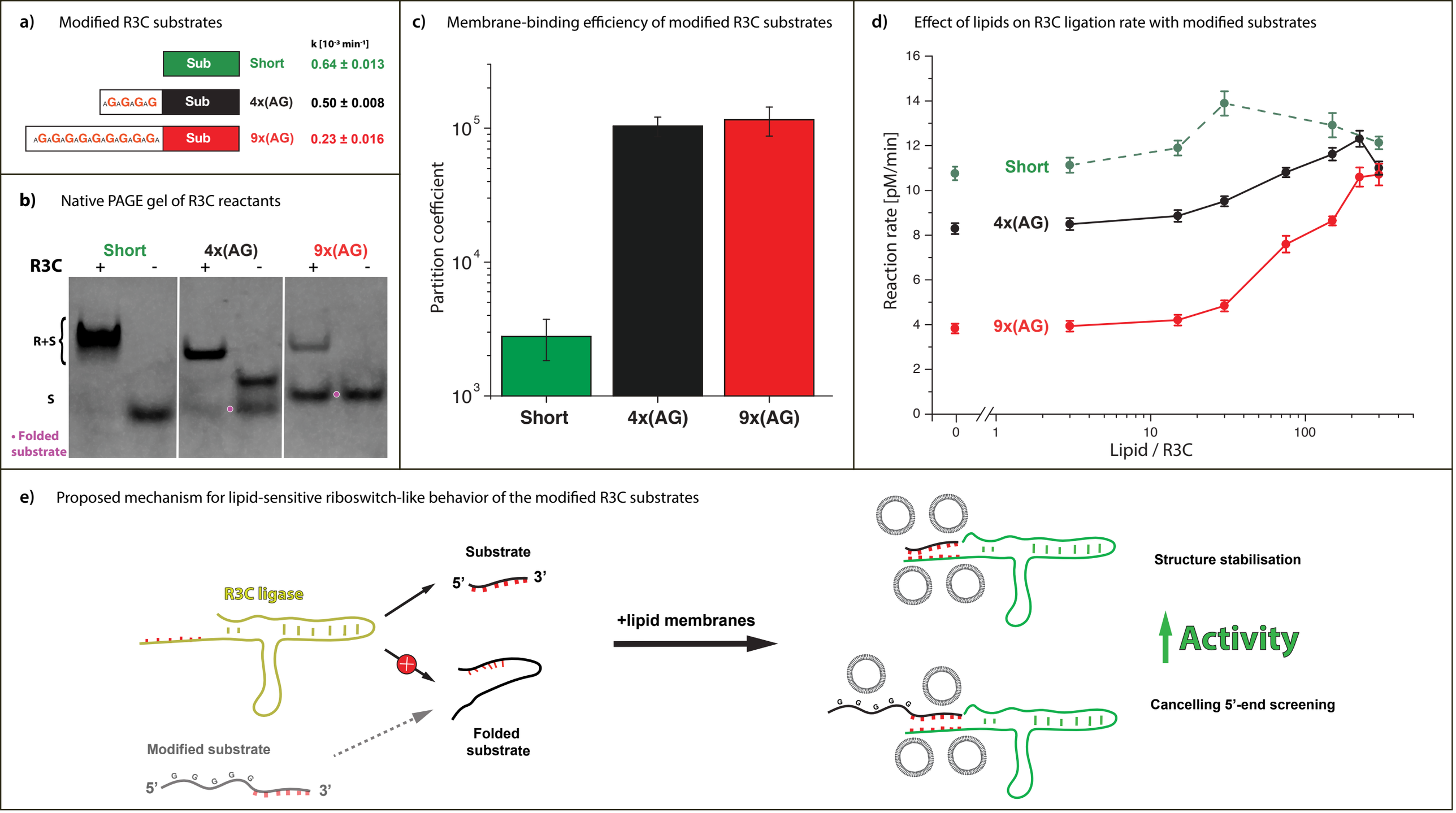

Fig. 6 Modification of the R3C substrate sequences enables lipid-dependent tunability of ligation rate. (a) Modified R3C reaction substrates were synthesized in order to increase binding to the membrane. The catalytic 3' end of the molecule was enriched with 5' tails with varying G content. Reactions for modified substrates showed lower reaction rate constants compared with the unmodified substrate. **(b)** The mechanism for inhibition of activity was evaluated by analysis of R3C reactants using native PAGE. The unmodified short substrate is entirely bound to the ligase, whereas AG-modified substrates show mobility abnormalities, which suggest substrate folding (magenta points). **(c)** Modification of the substrate sequence through addition of a 5' overhang increases binding to the membrane. **(d)** Addition of lipid membranes to reactions with the G-rich substrates increases reaction rates to the level of the unmodified substrate. **(e)** We propose that the decrease of R3C reaction rates in the presence of G-rich substrates is based on the inhibition of the catalytic part of the substrate by the 5' G-rich overhang. The presence of lipid membranes not only increases R3C-substrate stability, but also screens the 5'rich substrate part enabling the R3C reaction to proceed.